CrossMark

High temperature oxidation behavior of Ni-based superalloy GH586 in air

Jiang-Dong Cao, Jun-Song Zhang, Yin-Qun Hua*(i) **, Zhen Rong, Rui-Fang Chen, Yun-Xia Ye**

Abstract In this paper, the isothermal oxidation kinetics and oxidation behavior of GH586 superalloy from 800 to 1000 °C were investigated. The oxide scale morphologies of the surfaces and the cross sections after oxidation were characterized by means of X-ray diffraction (XRD) and scanning electron microscope (SEM) equipped with energy-dispersive spectroscopy (EDS). The results show that the growth of the oxide scales on the surface of superalloy GH586 obeys a parabolic law with the activation energy of 241.4 kJ·mol^{-1} from 800 to 1000 °C. The dense oxide scale formed at 800 °C is mainly composed of Cr_2O_3, $NiCr_2O_4$ and a small amount of TiO_2. At 900 °C, the oxide scale is divided into two layers: the outer layer with multiple cracks is mainly composed of Cr_2O_3 and TiO_2, while the inner is a layer of dense Cr_2O_3. Under the oxide scale, aluminum-rich oxides along the grain boundaries are generated by the internal oxidation. At 1000 °C for 100 h, cracks throughout the whole oxide film accelerate the oxidation rate of Ni-based superalloy GH586 and large blocks of TiO_2 in the oxide scale are generated, resulting in the spallation of oxide scale.

1 Introduction

Superalloys have been widely used in high temperature environments, such as aircraft engine blades, nuclear energy equipment and the petroleum industry, due to its excellent resistance to hot corrosion [1], fatigue [2] and oxidation [3, 4] at high temperatures. Among the various superalloy systems, Ni-based superalloys have good comprehensive properties, so they are widely used in a variety of high performance engine parts [5–7]. Ni-based superalloy GH586, when developed successfully, can serve between 750 and 850 °C [8]. It is often used in engine turbine disks of lox or kerosene rockets and the first stage turbine rotors of several new intercontinental missiles in China [9].

Oxidation resistance of superalloys depends on dense oxidation films on the surface of materials, which grow slowly and prevent oxygen from diffusing to the matrix [10]. It is well known that Al_2O_3, Cr_2O_3 and SiO_2 films with good thermodynamics stability at high temperatures are generated in the process of superalloys oxidation [11]. Owing to the different content of elements, the preparation process and chemical composition in superalloys, the oxidation behaviors of the superalloys are quite different. It is reported that the oxidation behaviors of superalloys were investigated by many scholars, such as Inconel 713 [12], MAR-M247 [13], DZ40 M [14] and GTD-111 [15]. According to these studies, whatever oxide films of superalloys will gradually spall with the increase of working temperature and time, this results in accelerating oxidation corrosion rate of superalloys significantly. In

J.-D. Cao, J.-S. Zhang, Y.-Q. Hua*, Z. Rong
School of Material Science and Engineering, Jiangsu University, Zhenjiang 212013, China
e-mail: huayq@ujs.edu.cn

J.-D. Cao
Mechanical and Electrical Department, Nantong Shipping College, Nantong 226010, China

R.-F. Chen, Y.-X. Ye
School of Mechanical Engineering, Jiangsu University, Zhenjiang 212013, China

order to find out the reasons for spallation of oxide scales, many researchers carried out plenty of work. It is well accepted that internal oxidation will take place to form the acicular morphology inner oxides during high temperature oxidation, which may be the initiation sites of cracks that result in the destruction of the oxide films with temperature and time increasing [16, 17]. Some elements in Ni-based superalloys, such as sulfur, carbon, titanium, etc., may form the corresponding compounds in grain boundaries [18, 19], the size of which can become larger with temperatures increasing, reducing the bonding strength between oxide scales and the matrix and destroying the continuity of oxidation films [20, 21]. Although the oxidation behaviors of a few superalloys were investigated, there are very few literatures on oxidation resistance of Ni-based superalloy GH586, and the further study on oxidation mechanism is needed.

In this paper, the high temperature oxidation behavior of Ni-based superalloy GH586 at 800, 900 and 1000 °C was investigated. The oxidation kinetics, the oxide scale composition, the surface and cross-sectional morphologies were elaborated. The growth and spallation mechanism of oxidation scales were revealed, providing a theoretical basis for practical engineering applications and failure analyses.

2 Experimental

2.1 Materials

The alloy used in this experiment was Ni-based superalloy GH586 (nominal composition: 19.00 wt% Cr, 11.00 wt% Co, 1.60 wt% Al, 3.20 wt% Ti, 8.00 wt% Mo, 3.00 wt% W, 0.06 wt% C, balanced Ni). It was dealt with precipitation strengthening and aging treatment. Figure 1 shows the microstructure of the superalloy GH586. From Fig. 1a, it can be seen that the superalloy grains have a fine equiaxed structure and distribute uniformly. According to Fig. 1d, e, the white chains in grain boundaries and blocks in grain interior in Fig. 1b are carbides, and they are respectively $M_{23}C_6$ and M_6C [8]. γ' phase which is the main strengthening phase in the alloy in Fig. 1c is almost 50–60 nm in size, and the morphologies seem approximately cuboid [13].

2.2 Oxidation experiments

Rectangular specimens with dimensions of 10 mm × 10 mm × 5 mm were cut from Ni-based superalloy GH586 by electrical discharge machining (EDM). The surfaces of these specimens were ground to 1200 mesh with
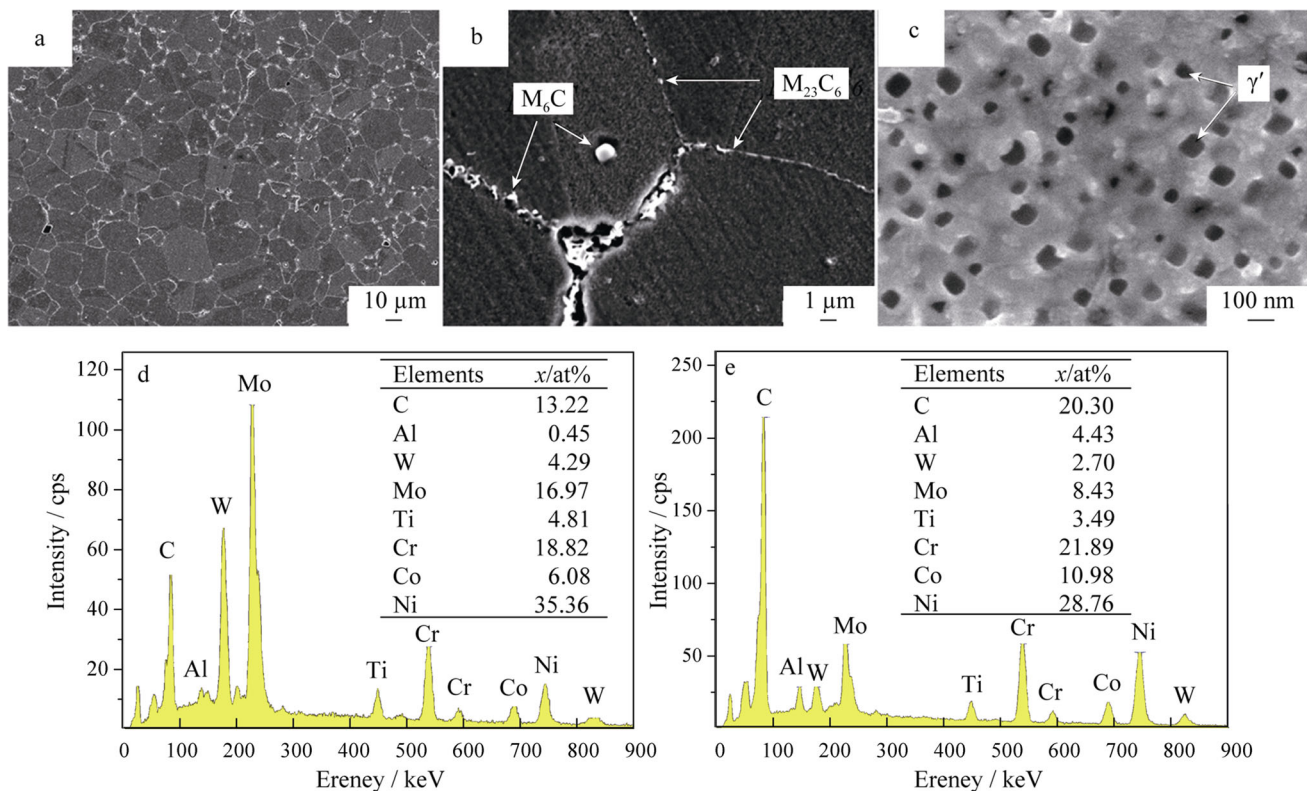

Fig. 1 SEM images of GH586 superalloy at room temperature: **a** metallographical structure, **b** carbides, and **c** γ' phase; EDS analysis of carbides: **d** $M_{23}C_6$ and **e** M_6C
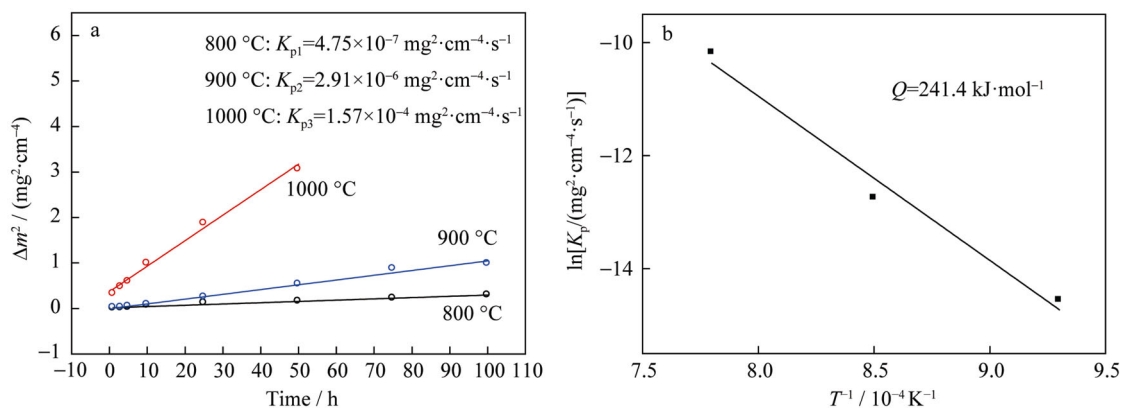
Fig. 2 Square of weight gain per unit area (Δm^2) versus time for Ni-based superalloy GH586 oxidized at temperature ranging from 800 to 1000 °C **a** and temperature dependence of parabolic rate constant for oxidation of Ni-based superalloy GH586 **b**

SiC sandpaper and polished before examination. The continuous-isothermal-mass-change measurements were performed from 800 to 1000 °C in air for 100 h. The specimens were suspended in a thermo balance with a Pt wire.

2.3 Microstructural analysis of oxide scale

After oxidation, the specimens were characterized. The phase composition of the oxide scale was measured by X-ray diffractometer (XRD, D8 Advance) with copper target at 3 kW in 2θ range of 10°–90°. The surface morphology and chemical composition of the oxide scale were investigated by scanning electron microscopy (SEM, JSM-7001F) equipped with an energy dispersive spectroscopy (EDS) system.

3 Results and discussion

3.1 Oxidation kinetics

Figure 2 shows the square of weight gain per unit area (Δm^2) as a function of time in the temperature range of 800–1000 °C in air. After oxidation at 900 °C for 100 h and 1000 °C for 50 h, the oxide scales on the surface just begin to spall. From the linear fit in Fig. 2a, it can be concluded that the oxidation of Ni-based superalloy GH586 from 800 to 1000 °C is in excellent agreement with a parabolic rate law. The parabolic rate constant (K_p) increases from 1.44×10^{-5} mg$^2\cdot$cm$^{-4}\cdot$s^{-1} at 800 °C to 4.81×10^{-5} mg$^2\cdot$cm$^{-4}\cdot$s^{-1} at 1000 °C.

The following equation indicates the temperature dependence of the parabolic rate constants.

$$K_p = K_0 \exp(-Q/RT) \tag{1}$$

where Q denotes oxidation activation energy which is energy barrier crossed during oxidation, K_0 is a constant

which can be obtained by solving equations, R is gas constant and T is temperature. According to the fitted line, the oxidation activation energy of Ni-based superalloy GH586 is 241.4 kJ·mol^{-1} from 800 to 1000 °C, as shown in Fig. 2b. It is close to the diffusion activation (259 kJ·mol^{-1}) of Cr^{3+} in oxide scale [22], indicating that the oxidation behaviors of superalloy GH586 are controlled by the diffusion of Cr^{3+} in oxide scale. It is almost in accordance with that of Ni-based superalloy K44 reported in Ref. [22].

3.2 Composition of oxide scale

Figure 3 shows XRD patterns of oxide scales of GH586 superalloy oxidized at 800, 900 and 1000 °C for 100 h. After oxidation at 800, 900 and 1000 °C for 100 h, the compositions of oxide scale on the surface are basically the same, but the relative content of each constituent phase changes. The oxide films at different temperatures consist of Cr$_2$O$_3$, spinels NiCr$_2$O$_4$ and TiO$_2$. The diffraction peak
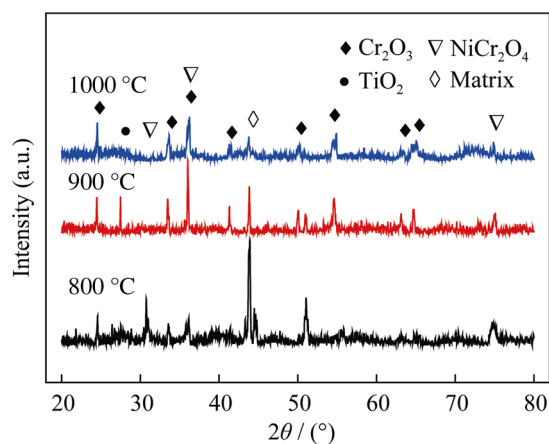

Fig. 3 XRD patterns of oxide surfaces on Ni-based superalloy GH586 samples oxidized from 800 to 1000 °C for 100 h

of the matrix is stronger after oxidation at 800 °C for 100 h, illustrating that the formed oxide film is thin. The base peak becomes weaker and the thickness of oxide film increases with temperature increasing. The peak of TiO_2 is not obvious, while Cr_2O_3 and $NiCr_2O_4$ peaks are relatively strong. It is shown that the film formed at 800 °C is mainly composed of Cr_2O_3, $NiCr_2O_4$ and a small amount of TiO_2. At 900 °C, the peaks of all the constituent phases in the film are significantly enhanced, and the TiO_2 peak is strong. When the temperature rises to 900 °C, Cr_2O_3 and $NiCr_2O_4$ in oxide film form a thicker oxide film which contains a large amount of TiO_2. The titanium oxide coarsens and makes the oxide scale loose, reducing the density of the outer layer of oxide film at the initial stage of oxidation [14]. The weak TiO_2 peak at 1000 °C is caused by the peeling of the bulk pre-formed TiO_2 oxidation layer, and the inner Cr_2O_3 is exposed, resulting in further oxidation of the alloy. Moreover, there are a small amount of $NiCr_2O_4$ oxides which would consume a little Cr element that can be supplied to oxide scale with temperature increasing.

3.3 Surface and cross-sectional morphology of oxide scale

Figure 4a–c shows surface morphologies of oxide scale at 800, 900 and 1000 °C, respectively. Different surface morphologies could be observed, and the grain size of the oxides increases with temperature increasing. A dense oxide scale with well-shaped crystallites is observed for the sample oxidized at 800 °C. EDS and XRD analyses show that the oxide is mainly composed of Cr_2O_3, TiO_2 and $NiCr_2O_4$. As shown in Fig. 4a, the small white oxide is TiO_2. Ti content of oxide scale at 900 °C for 100 h is more than that at 800 °C for 100 h (Fig. 4d, e), meanwhile, Cr content decreases obviously. These titanium oxides would agglomerate into coarse particles with time gradually increasing, which makes the outer oxide film loose and provides the channel for oxygen diffusing into substrate. In Fig. 4c, f, it is found that a lot of holes in outer oxide film are formed and Ti content was decreases greatly, which results from the large oxide scale spalled. With time increasing at 1000 °C, TiO_2 forms large particles and destroys the continuity of the oxide film; moreover, the spinels $NiCr_2O_4$ generated in the process of oxidation consume a great quantity of Cr elements in oxide film, leading to less Cr_2O_3 than that at 900 °C. In addition, from Fig. 4d–f, it can be seen that a small amount of aluminum oxides in oxidation scales are found, and Al content is almost unchanged. Owing to its low content, a dense and continuous aluminum oxide scale could not be formed. Therefore, only the dense Cr_2O_3 layer protects the matrix effectively in the process of oxidation rather than aluminum oxide.

With the increase of oxidation temperature for 100 h, the diffusion rate of Ti^{4+} in the alloy speeds up, leading to the rapid growth of TiO_2, and thicker grains of TiO_2 are formed at 900 °C than at 800 °C. After oxidation at
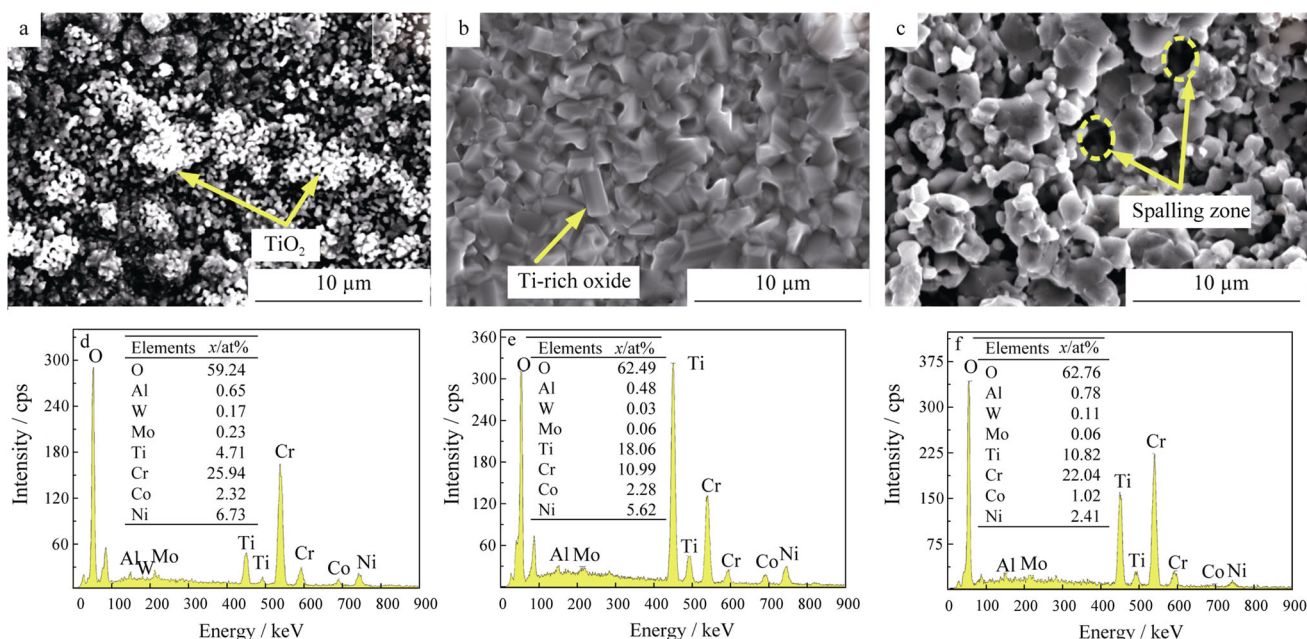

Fig. 4 SEM images of surface morphologies of oxidation films after oxidation and corresponding EDS result of oxide scales at **a**, **d** 800 °C, **b**, **e** 900 °C and **c**, **f** 1000 °C

1000 °C for 100 h, TiO_2 particles are spalled and then destroy the continuity of the protective Cr_2O_3 film, resulting in the decrease in oxidation resistance of the superalloy [15, 16].

Figure 5a–c show cross-sectional morphologies of GH586 superalloy after oxidation at 800, 900 and 1000 °C for 100 h, Fig. 5d–f shows elemental profiles in a cross section with distance from oxidation surface. It is seen from Fig. 5a, d that a layer of dense oxide film with 3 μm in thickness is formed on the surface of superalloy GH586 oxidized at 800 °C for 100 h. According to XRD analysis, the oxide film is mainly composed of Cr_2O_3, $NiCr_2O_4$ and a small amount of TiO_2. Meanwhile, a few aluminum oxides are found at the bottom of the oxidation scales, and a small amount of aluminum-rich oxides (Al_2O_3) exist in the grain boundaries due to the internal oxidation of aluminum, and the depth of the internal oxidation is about 3–4 μm. In Fig. 5b, e, the thickness of the surface oxide film increases to 10 μm after oxidation at 900 °C for 100 h, and the film can be divided into two layers. The outer layer with 5 μm in thickness becomes looser than the inner, and the depth of the internal oxidation is up to 15–16 μm according to the change of aluminum oxides in cross section. In Fig. 5c, f, the oxide scale develops into a layer structure after oxidation at 1000 °C for 100 h. It is seen that aluminum oxides exist at the deeper locations caused by the severer internal oxidation and the depth of the rich-aluminum oxides in the grain boundaries reaches around 40 μm. But the thickness of the oxide scale decreases to about 12 μm, this is because of the outer oxide film spalled in multiple areas, leading to the great decrease of Ti content in cross section. Meanwhile, the element Cr in substrate diffuses outward to generate a small amount of new Cr_2O_3. Moreover, it is easily seen that Ni content decreases greatly after oxidation at 900 °C for 100 h, and it is almost 0 after oxidation at 1000 °C for 100 h, as shown in Fig. 5d–f, which is caused by the appalling spinels $NiCr_2O_4$ in oxide scales.

Figure 6 shows EDS results of outer layer, inner layer and internal oxidation region of GH586 superalloy after oxidation at 900 °C for 100 h. As shown in Fig. 6a, many cracks form in outer layer, which are caused by the large blocks of TiO_2. Through these cracks, oxygen is easily propagated into the matrix and forms aluminum-rich oxides (Al_2O_3) along grain boundaries. Meanwhile, Fig. 6b shows that inner layer is a layer of dense Cr_2O_3, including a small amount of TiO_2. The internal oxidation of aluminum beneath the oxide scale is generated along grain boundaries, as its EDS is shown in Fig. 6c. Owing to the low aluminum concentration in the alloy, it is not enough to form a continuous oxide film on Al_2O_3. The internal oxide along grain boundaries can help to connect oxide scale at the interface with the matrix, and form a continuous oxide zone at some locations to improve the adhesion of oxide scale effectively [17, 18].
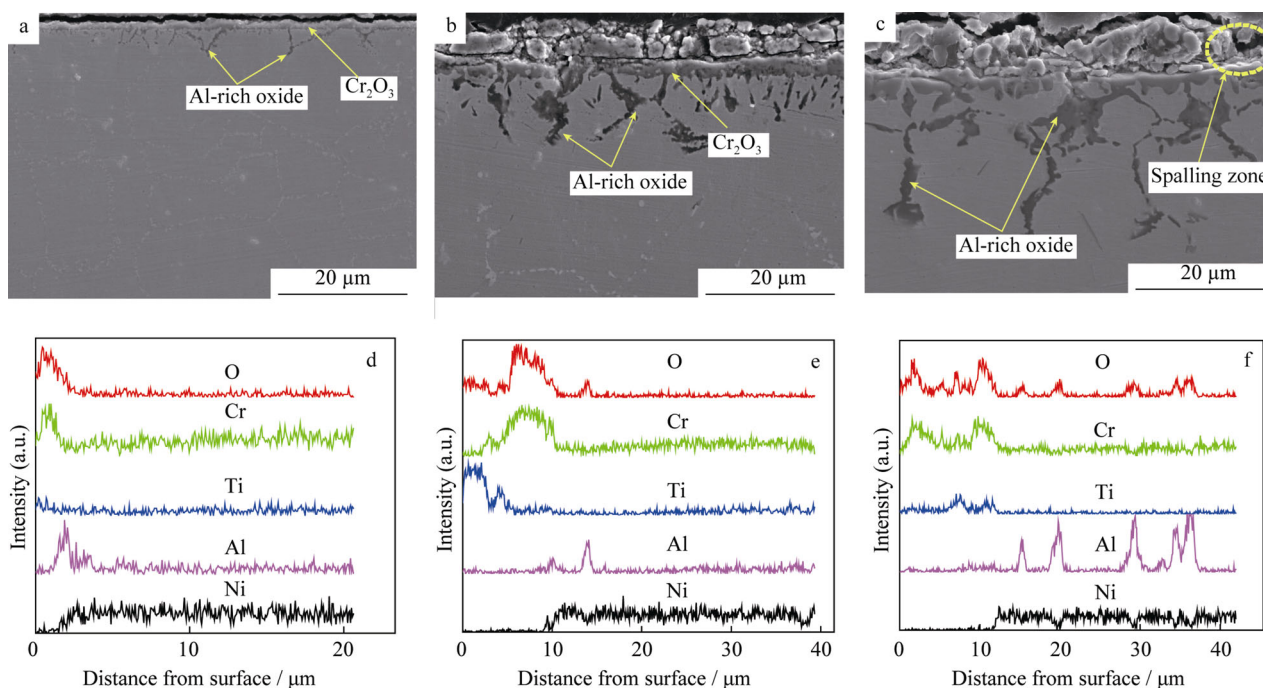

Fig. 5 SEM images of cross-sectional morphologies of superalloy for 100 h and corresponding concentration profiles of elements from oxidation surface oxidized at **a**, **d** 800 °C, **b**, **e** 900 °C and **c**, **f** 1000 °C
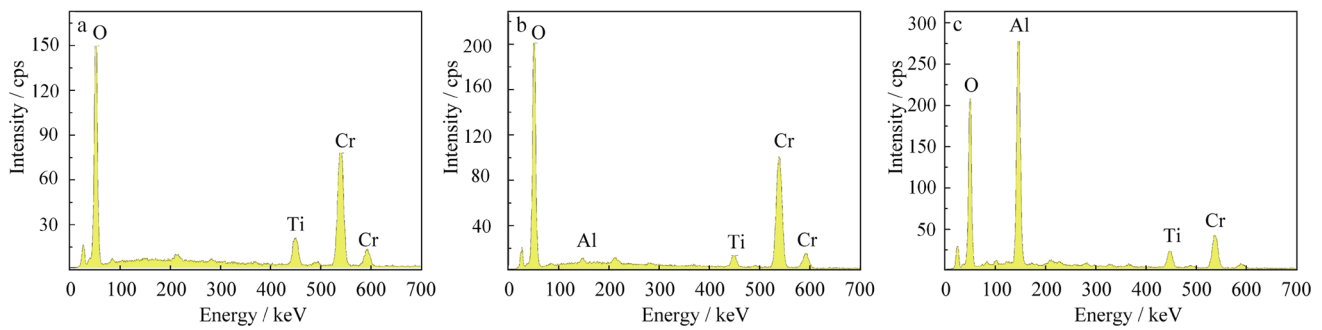
Fig. 6 EDS results of **a** outer layer, **b** inner layer and **c** internal oxidation region at 900 °C for 100 h

3.4 Discussion

Figure 7 shows the evolution of oxide scale on superalloy GH586 exposed to air from 800 to 1000 °C for 100 h. At the first stage of nucleation, mechanical failure of the initial passive layer might take place, thus leading to the nucleation and growth of initial Cr oxide encountering with O^{2-}, resulting from the decomposition of oxygen absorbed at the surface of the superalloy. $X = 0$, which is slightly beneath the initial chromium oxide, is the initial surface of the superalloy as the chromium oxide layer grows by countercurrent diffusions of chromium and oxygen. The consistency and integrity of the initial chromium oxide layer depend on the content of the superalloy composition. The slowest kinetic should be attributed to the formation of the chromium oxide layer, which may hinder the diffusion of cations and anions during the first stage of oxidation on the superalloy. Meanwhile, some small titanium oxide particles and Ni–Cr spinels in chromium oxide layer are formed near interface. Owing to the diffusion of only a small amount of oxygen atoms into substrate, the slight internal oxidation along grain boundaries produces a little Al_2O_3.

Owing to that the diffusion rate of Ti^{+4} is faster than that of Cr^{3+} under the same conditions [19], titanium oxides (TiO_2) transfer to outer layer of oxide film, and titanium oxides grow up gradually with temperature increasing, resulting in that the outer layer of oxide scale becomes relatively loose at 900 °C. It provides the channels for the diffusion of oxygen and accelerates the internal oxidation along grain boundaries. Moreover, the amount and size of Ni–Cr spinels ($NiCr_2O_4$) in oxide film increase with temperature increasing, and $NiCr_2O_4$ consumes a part of Cr^{3+} diffusing from the matrix, resulting in that the oxidation layer is not able to obtain enough supplement of Cr^{3+} [21–24]. The inner layer of oxidation film is still compact and integrity, and continues to protect the matrix. At 1000 °C, titanium oxides grow into plenty of large blocks which destroy the continuity of the oxide film. The oxide scales in multiple areas are spalled under the action of thermal stress, it may provide the channels for oxygen to diffuse into the matrix, accelerate the oxidation process and reduce the resistance of high temperature oxidation.

The high temperature oxidation resistance of superalloys should be attributed to the chemical compositions of the superalloy, especially the contents of chromium (18–20) wt% [25], which has been studied quite extensively. When chromium content is higher than 15 wt%, it can form thin composite oxide films mainly containing Cr_2O_3, $NiCr_2O_4$ and TiO_2, which can prevent further oxidation of alloys [4].
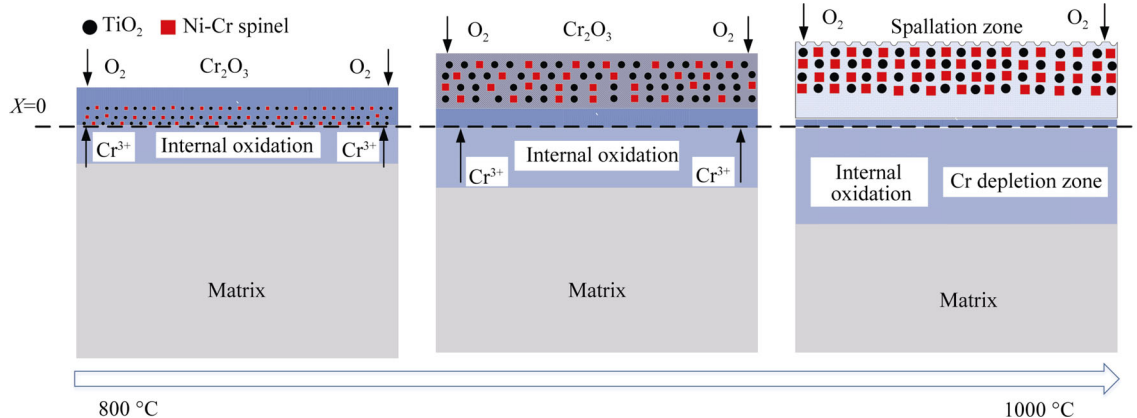

Fig. 7 Oxide scale evolution on surfaces of superalloy GH586 exposure to air from 800 to 1000 °C for 100 h

This evolution process of the oxide film is primarily controlled by ion diffusion [26–28]. Although Cr_2O_3 film prevents the further oxidation of the elements in the alloy, the grown up titanium oxide in the film with temperature and time increasing makes the oxide film more loose; thus it provides channels for oxygen to diffuse into the matrix through oxide film and accelerates the internal oxidation of the superalloy [29, 30].

4 Conclusion

The oxidation kinetics curves follow the parabolic law with the activation energy of 241.4 kJ·mol^{-1}. The oxide scale on the surface of Ni-based superalloy GH586 is composed of Cr_2O_3, $NiCr_2O_4$ and a small mount of TiO_2. With temperature increasing, TiO_2 particles gradually grow up and destroy the continuity of oxide film. Moreover, the spinels $NiCr_2O_4$ generated in the process of oxidation greatly consume Cr element in oxide film, which cannot obtain enough supplement of Cr element from the matrix for the oxide scale. At 900 °C, the oxide scales display two layer structures: the outer layer of the oxide films consists of Cr_2O_3, $NiCr_2O_4$ and TiO_2, while the internal oxidation occurs under the oxide film and generates rich-aluminum oxides. At 1000 °C for 100 h, the cracks throughout the oxide film accelerate the oxidation rate of Ni-based superalloy GH586. Meanwhile, TiO_2 forms into large blocks and accelerates the oxidation scale spalling.

References

[1] Wang J, Zhou LZ, Sheng LY. The microstructure evolution and its effect on the mechanical properties of a hot-corrosion resistant Ni-based superalloy during long-term thermal exposure. Mater Des. 2012;39(39):55.
[2] Yuan SH, Wang YR, Wei DS. Experimental investigation on low cycle fatigue and fracture behavior of a notched Ni-based superalloy at elevated temperature. Fatigue Fract Eng Mater Struct. 2014;37(9):1002.
[3] Liua CT, Mab J, Sunc XF. Oxidation behavior of a single-crystal Ni-base superalloy between 900 and 1000 °C in air. J Alloys Compd. 2010;491(S1–2):522.
[4] Ning LK, Zheng Z, An FQ, Tang S, Tong J. Thermal fatigue behavior of K125L superalloy. Rare Met. 2016;35(2):1–5.
[5] Fei M. Researching on high-temperature oxidation property of NiCrAlY coatings on nickel-base superalloy K465. Harbin: Harbin Engineering University; 2012. 1.
[6] Wu XC. Research on high-temperature oxidation property of calorized coating on GH907 superalloys. Harbin: Harbin Engineering University; 2011. 1.
[7] Gao L. Research for high temperature oxidation properties of aluminized coating on K438 superalloy. Harbin: Harbin Engineering University; 2004. 1.
[8] Shi CX. High Temperature Materials Branch of Chinese Society for Metals, China Superalloys Handbook. Beijing: China Standard Press; 2012. 818.
[9] Hua YQ, Rong Z, Ye YX. Laser shock processing effects on isothermal oxidation resistance of GH586 superalloy. Appl Surf Sci. 2015;330(6):439.
[10] Wu MY, Chen MH, Zhu SL, Wang FH. Effect of sand blasting on oxidation behavior of K38G superalloy at 1000C. Corros Sci. 2015;92:256.
[11] Wang CJ, Chen SM. Microstructure and cyclic oxidation behavior of hot dip aluminized coating on Ni-base superalloy Inconel 718. Surf Coat Technol. 2006;201(7):6601.
[12] Albert B, Völkl R, Glatzel U. High-temperature oxidation behavior of two nickel-based superalloys produced by metal injection molding for aero engine applications. Metall Mater Trans A. 2014;45A(10):4561.
[13] Weng F, Yu HJ, Chen CZ, Wan K. High-temperature oxidation behavior of Ni-based superalloys with Nb and Y and the interface characteristics of oxidation scales. Surf Interface Anal. 2015;47(3):362.
[14] Liu PS, Liang KM. High-temperature oxidation behavior of the Co-base superalloy DZ40 M in air. Oxid Met. 2000;53(3):351.
[15] Yun DW, Seo SM, Jeong HW, Yoo YS. The cyclic oxidation behaviour of Ni-based superalloy GTD-111 with sulphur impurities at 1100 °C. Corros Sci. 2014;90:392–401.
[16] Cruchley S, Taylor MP, Evans HE. Characterisation of subsurface oxidation damage in Ni based superalloy. Mater Sci Technol. 2014;30(15):1884.
[17] Geng L, Na YS, Park NK. Oxidation behavior of alloy 718 at a high temperature. Mater Des. 2007;28(3):978.
[18] Guo JT. Materials Science and Engineering for Superalloys (Vol. 1). Beijing: Sciences Press; 2008. 4.
[19] Xu GH. Study on hot-working parameters and heat treatment of GH586 superalloy. Shenyang: Northeastern University; 2004. 40.
[20] Zhu LJ, Zhu SL, Wang FH, Zhang JQ. Comparison of the cyclic oxidation behavior of low expansion Ni+Cr AlYSiN nanocomposite and a NiCrAlYSi coating. Corros Sci. 2014;80(3):393.
[21] Wang MQ, Qu JL, Yin TZ, Sheng JY. Study on oxidation behavior of alloy GH4720Li at high temperatures. J Iron Steel Res. 2010;22(9):28.
[22] Li Y. High-temperature oxidation, hot corrosion of five Ni-base superalloys and their protection. Shenyang: Northeastern University; 2004. 35.
[23] Liang JC, Zhou WP, Zhang FG, Mu JG, Zhao HB. Evolution analysis of existing forms of Ti and Al elements during preparation of TiAlN coating. Chin J Rare Met. 2014;38(4):561.
[24] Cao H, Peng CZ, Yang T, Xiang L, Xiong W. Microstructure and high temperature oxidation behavior of $Cu_{30}Ni_{10}Cr_8A_{12}Zr$ alloy. Chin J Rare Met. 2014;38(6):1121.
[25] Birks N, Meier GH. Introduction to high temperature oxidation of metals. Beijing: High Education Press; 2010. 120.
[26] Ren X, Wang FH, Wang X. High-temperature oxidation and hot corrosion behaviors of the NiCr+CrAl coating on a nickel-based superalloy. Surf Coat Technol. 2005;198(S1–3):425.
[27] Yun DW, Seo SM, Jeong HW, Yoo YS. The effects of the minor alloying element Al, Si and Mn on the cyclic oxidation of Ni–Cr–W–Mo alloys. Corros Sci. 2014;83(3):176.
[28] Zhang S, Wang Q, Zhao XS, Zhang CH. High temperature oxidation behavior of cast Ni-based superalloy K444. J Shenyang Univ Technol. 2010;32(2):136.

[29] Wang L, Pan LL, Peng H, Guo HB, Gong SK. Cyclic oxidation behavior of Cr-/Si-modified NiAlHf coatings on single-crystal superalloy produced by EB-PVD. Rare Met. 2016;35(5):1–5.

[30] Fang L, Liu XG, Li Y, Yuan C, Guo JT. Oxidation kinetics of cast Ni-base superalloy K44. J Shenyang Inst Chem Technol. 2004;18(2):121–4.